Hindawi Publishing Corporation
International Journal of Antennas and Propagation
Volume 2012, Article ID 735080, 6 pages
doi:10.1155/2012/735080

Research Article

Diversity Gain through Antenna Blocking

V. Dehghanian, J. Nielsen, and G. Lachapelle

Position, Location, and Navigation Group, University of Calgary, 2500 University DR NW, Calgary AB, Canada T2N 1N4

Correspondence should be addressed to V. Dehghanian, vdehghan@ucalgary.ca

Received 6 July 2011; Accepted 19 October 2011

Academic Editor: Byungje Lee

As part of the typical usage mode, interaction between a handheld receiver antenna and the operator's RF absorbing body and nearby objects is known to generate variability in antenna radiation characteristics through blocking and pattern changes. It is counterintuitive that random variations in blocking can result in diversity gain of practical applicability. This diversity gain is quantified from a theoretical and experimental perspective. Measurements carried out at 1947.5 MHz verify the theoretical predictions, and a diversity gain of 3.1 dB was measured through antenna blocking and based on the utilized measurement setup. The diversity gain can be exploited to enhance signal detectability of handheld receivers based on a single antenna in indoor multipath environments.

1. Introduction

Temporal signal fluctuation arising from user interaction with a handheld device in the form of motion and signal blocking in a multipath environment poses a formidable challenge to the performance of wireless communication. Antenna diversity based on employing multiple antennas with different radiation characteristics has long been in use in diversity systems and have proven effective in mitigating multipath fading [1, 2]. Nevertheless, the size of a multielement antenna array is not compatible with the small physical size constraint of a handheld terminal.

In pattern diversity systems, signals at the output of antennas with orthogonal patterns are statistically uncorrelated [3, 4]. More recently, pattern diversity based on arrays of closely spaced active and parasitic elements has been investigated for use in handheld devices [5–9]. Pattern diversity based on closely spaced antenna elements is attractive for use in handheld terminals due to smaller array dimensions. Use of parasitic elements for steering antenna patterns based on switching the parasitic elements on and off is discussed in [6, 9]. A variant technique based on terminating the parasitic elements to different impedances which allows for more flexible antenna patterns and a higher-resolution diversity optimization is discussed in [5].

In the typical usage mode of a handheld unit, random temporal changes of signal blockage occur naturally as the user interacts with the device. Analysis and consequences of such interaction are varied as described in [10] for different hand grips and handheld-head positions [11–13] which affect the antenna radiation pattern. Blocking, coupling, diffraction, and refraction of elecrtromagnetic (EM) waves due to objects in the close proximity of a handheld antenna also result in variability in antenna radiation characteristics. Such variations in the handset antenna pattern are conventionally regarded as being detrimental as they result in signal decorrelation limiting the processing gain achievable by coherent signal integration. However, motion and the corresponding variation in orientation and signal blocking can be exploited to achieve usable diversity gain based on forming a synthetic array [14–17]. This variability of the antenna blocking and consequential potential diversity gain is analyzed and demonstrated through experimental results in this paper. As will be shown, variations in signal blocking are another means of realizing diversity gain.

The remainder of this paper is organized as follows. Section 2 presents the theoretical analysis of antenna blocking. Section 3 defines the diversity gain analysis technique and the system model. A case study is also discussed in Section 3 . Section 4 presents the measurement results and Section 5 the conclusions.

2. Theoretical Analysis of Antenna Blocking

Vicinity of a handheld antenna to external objects, for example, operator's body, metallic doors, tinted windows, and so forth, affects several of antenna properties. Electromagnetic (EM) waves impinging on a receiver antenna in the proximity of an object go through a variety of propagation mechanisms, for example, attenuation, scattering, and diffraction. Signal attenuation through blocking of multipath rays arriving from the direction a blocking object can be construed as variation in antenna radiation pattern. This variation in antenna radiation pattern results in signal decorrelation which can be exploited to achieve usable diversity gain in harsh multipath environments such as indoors.

Copolarized antennas are assumed at the transmitter and the receiver ends. A uniform sphere of scatterers is considered to be a suitable model for representing the indoor multipath [18, 19]. Consequently, the time averaged normalized transmit power density is assumed to be distributed uniformly in terms of the bearing, Ω, such that the distribution of normalized incident signal, $\mathbf{E}_s(\Omega)d\Omega$, follows from

$$\mathbf{E}_s(\Omega,t)d\Omega = \frac{1}{4\pi}d(t)s_0(t)d\Omega\hat{\theta}, \tag{1}$$

where $s_0(t)$ is the modulating signal, $\hat{\theta}$ is the polarization unit vector of the transmit signal which is assumed to be the same as the polarization of the receiving antenna, and $d(t) = 1$ is the normalized data component which is assumed to remain unchanged for the duration of signal sampling and as such will be suppressed in the remainder of this paper. The latter assumption is valid where a PILOT signal is available as in the case of CDMA IS95 [20] or where the data bits can be removed as in the case of assisted GPS scenarios [21]. Following Collin and Zucker [22] the open-circuit voltage, V, induced at an antenna output can be found from

$$V = \int \mathbf{E}(\Omega)\cdot\mathbf{E}_{s_{\text{bb}}}(\Omega)d\Omega, \tag{2}$$

where $\mathbf{E}_{s_{\text{bb}}}(\Omega)d\Omega = d\Omega\int s_0^*(t)\mathbf{E}_s(\Omega,t)dt$ is the baseband incident field arriving from $d\Omega$ and $\mathbf{E}(\Omega) = \mathbf{E}(\theta,\varphi) = E_\theta(\theta,\varphi)\hat{\theta}$ is the antenna's normalized far-zone radiated electric field which is also known as the vector effective length (VEL) as defined in [23]. Consequently, the normalized baseband signal at receiver's correlator output can be found from

$$\begin{aligned} s_i &= \int_{(i-1)\Delta T}^{i\Delta T} s_0^*(t)\left[\oint \beta_i(\Omega)\mathbf{E}(\Omega)\cdot\mathbf{E}_s(\Omega,t)d\Omega\right]dt, \\ &= \int_{(i-1)\Delta T}^{i\Delta T} s_0^*(t)s_0(t)dt\left(\frac{1}{4\pi}\oint \mathbf{E}(\Omega)\beta_i(\Omega)d\Omega\right), \\ &= \frac{\sigma_s}{4\pi M}\oint \mathbf{E}(\Omega)\beta_i(\Omega)d\Omega, \quad i=1,\ldots,M, \end{aligned} \tag{3}$$

where $\mathbf{E}(\Omega)$ is the normalized antenna electric field in the far field, $\beta_i(\Omega) = a(\Omega)\exp(j\psi(\Omega))$ is the isolated effect of blocking with $a(\Omega)$ as the attenuation of the arriving wave in the direction of elevation and azimuth angles (θ,φ), and $\psi(\Omega)$ as the excess phase shift resulting from blocking. In (3), the normalization $\int_{(i-1)\Delta T}^{i\Delta T}|s_0(t)|^2dt = \sigma_s/M$ is assumed such that $(\sigma_s/M)^2$ represents the average received signal power captured by an isotropic antenna after ΔT seconds of integration during the ith sampling subinterval, $(i-1)\Delta T \le t < i\Delta T$. Note that the test antenna is assumed to remain static for the duration of signal sampling denoted by signal snapshot period, T, which is divided into M sampling subintervals with durations $\Delta T = T/M$.

Following [3, Equation 29] and by taking into account (3), the cross-covariance between signal samples s_i and s_k can be found from

$$[\mathbf{C_s}]_{ik} = \frac{\sigma_s^2}{4\pi M^2}\oint P(\Omega)\beta_i(\Omega)\beta_k^*(\Omega)d\Omega, \quad i,k=1,\ldots,M, \tag{4}$$

where "$*$" denotes a complex conjugate and $P(\Omega) = |\mathbf{E}(\Omega)|^2$ is the normalized antenna power pattern. Note that in (4) the antenna itself is static during the signal measurement interval T such that any resulting diversity gain can be attributed solely to variations in the pattern blocking. As will be shown in the next section, the signal decorrelation arising from antenna blocking can be utilized to generate useful diversity gain.

3. Diversity Gain Analysis

3.1. System Model. While the analysis and algorithms in this paper are generic, the CDMA signal acquisition is considered as a test case for quantifying the achievable diversity gain. Acquisition of the received pilot signal is the initial processing of the CDMA mobile receiver which is typically based on some form of multihypothesis testing [24]. The design of the detection algorithm is based on target values of the probability of detection (P_D) and the probability of false alarm (P_F) associated with the search hypothesis. Consequently, the problem is modeled as one of choosing between H0, the noise-only hypothesis, and H1, the signal present hypothesis as

$$\begin{aligned} \mathbf{x} &= \mathbf{w} \quad \text{under H0}, \\ \mathbf{x} &= \mathbf{s}+\mathbf{w} \quad \text{under H1}, \end{aligned} \tag{5}$$

where $\mathbf{s} = [s_1,\ldots,s_M]^\dagger$ represents the Rayleigh faded signal samples distributed according to $\mathbf{s}\sim CN(\mathbf{0},\mathbf{C_s})$ with $CN(\boldsymbol{\mu},\mathbf{C})$ denoting a complex normal distribution with a mean of $\boldsymbol{\mu}$ and a covariance of $\mathbf{C}$. "$\dagger$" denotes a matrix transpose operation. $\mathbf{w} = [w_1,\ldots,w_M]^\dagger$ contains the white Gaussian noise samples distributed according to $CN(\mathbf{0},(\sigma_0^2/M)\mathbf{I}_M)$, where $\mathbf{I}_M$ is the M by M identity matrix and σ_0^2 is the intrinsic noise variance after T seconds of integration. Signal and noise are assumed to be independent. In addition, noise is assumed to be intrinsic such that blocking does not affect the noise power. Radiated noise results in higher diversity gain as blocking reduces the received noise power.

Consequently, the measured P_F and P_D quantify the performance of the diversity system through

$$P_F(\gamma) = 1 - \mathcal{F}(\gamma)\big|_{\mathrm{H0}},$$
$$P_D(\gamma) = 1 - \mathcal{F}(\gamma)\big|_{\mathrm{H1}}, \tag{6}$$

where $\mathcal{F}$ is the cumulative distribution function (CDF) of the combiner output under H0 or H1 and γ is the threshold [25]. Assuming that the statistics of the signal and noise components are known, the radio operating characteristic (ROC) curve of the antenna blocking diversity system maps any target P_{F0} to a P_{D0} through an onto transformation for a realization of average SNR, $\eta_M = \sigma_s^2/\sigma_0^2$ where σ_s^2 is the signal variance after a coherent integration of T seconds as seen from a nonblocked isotropic receive antenna and σ_0^2 is defined earlier. Conversely, in a nonblocked stationary antenna system, the detection requirement $\{P_{F0}, P_{D0}\}$ then maps into a required average SNR, η_1. Consequently, a quantitative metric of performance enhancement can be given by [14, 15, 26]

$$G|_{(P_{F0},P_{D0})} = 10\log_{10}\left(\frac{\eta_1}{\eta_{\mathrm{M}}}\right). \tag{7}$$

Note that the communication channel and the distribution of scatterers are assumed to remain static during the signal snapshot period. In this paper flat fading is assumed as the derivations are simplified while capturing the essence of the diversity gain based on pattern diversity.

3.2. Case Study. The impetus of this paper is to study the realizable processing gain based on antenna blocking. Therefore, a simple blocking scenario is assumed while other propagation mechanisms, for example, diffraction, refraction, and so forth, are not considered. A simple model is essential since it simplifies the analysis and provides insight to the rather counterintuitive problem of producing diversity gain based on antenna blocking.

A blocking scenario based on an isotropic antenna surrounded by a uniform sphere of scatterers, (8), and M uniform but mutually orthogonal blocking functions is considered. The blocking functions are

$$\beta_i = \begin{cases} \dfrac{1}{\sqrt{M}} & \Omega_i, \\ 0 & \text{other}, \end{cases} \qquad i = 1, \ldots, M, \tag{8}$$

where Ω_i is $1/(4\pi M)$ steradians wide. The signal covariance matrix can be found by replacing (8) in (4) as

$$[\mathbf{C_s}]_{ik} = \frac{\sigma_s^2}{4\pi M^2}\left(\frac{\delta(i-k)}{M}\right)\oint P(\Omega)d\Omega = \left(\frac{\sigma_s^2}{M^3}\right)\delta(i-k), \tag{9}$$

where $\delta(\cdot)$ is the Delta function and the normalization, $\oint P(\Omega)d\Omega = 4\pi$, is assumed. The obtained signal samples, $\mathbf{x}$, can be combined using a square-law combiner (SLC) as

$$z_{\mathrm{SLC}} = \underline{\mathbf{X}}^{\mathrm{H}}\underline{\mathbf{X}} = \sum_{i=1}^{M}|x_i|^2. \tag{10}$$

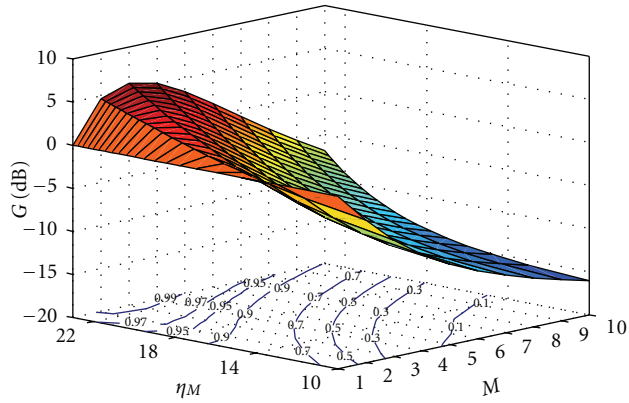

Figure 1: Achievable processing gain based on antenna blocking with M orthogonal blocking functions, $P_{F0} = 0.01$, and various values of available SNR (η_M). The contour curves show the corresponding P_{D0}.

z_{SLC} is distributed according to

$$\mathrm{f}_z(\gamma) = \begin{cases} \chi^2_{2M}(M\gamma) & : \mathrm{H0}, \\ \chi^2_{2M}\left(\dfrac{M\gamma}{\sigma_s^2/M^2+1}\right) & : \mathrm{H1}, \end{cases} \tag{11}$$

where $\chi^2_{2M}(\gamma/\sigma^2)$ denotes a central chi-square probability density function (PDF) with $2M$ degrees of freedom and variance of individual Gaussian components, σ^2 [25]. Consequently, the realizable diversity gain can be computed by integrating the PDF of (11) and utilizing (6) and (7). Figure 1 shows the realizable diversity gain for various values of M, different realizations of η_M, and a practical $P_{F0} = 0.01$. The achievable processing gain, G, is a combination of the increasing diversity gain, arising from signal decorrelation, as well as the decreasing signal power, as M increases. Note that the decrease in the signal power arises from shorter integration times, ΔT, and larger blockings for larger M. Consequently, for any value of η_M, there is a value of M that corresponds to the highest processing gain as is evident from Figure 1. As can be seen from Figure 1, antenna blocking is detrimental in low SNR regimes. On the other hand, blocking results in a net processing gain for higher SNR. The contour plots of Figure 1 show the corresponding P_{D0} for the given $P_{F0} = 0.01$, η_M, and M. Note that higher probabilities of detection correspond to higher processing gains that happen at higher values of SNR.

4. Experiments and Results

A set of measurements was conducted to validate the analytical results of the previous section. The measurement site was a typical one-story laboratory with a variety of equipment and was verified to typify a Rayleigh fading channel [16]. The experimental setup is shown in Figure 2.

The CDMA pilot signal transmitted from an outdoor base station at 1947.5 MHz was captured by a half-wavelength dipole antenna. The test antenna was then

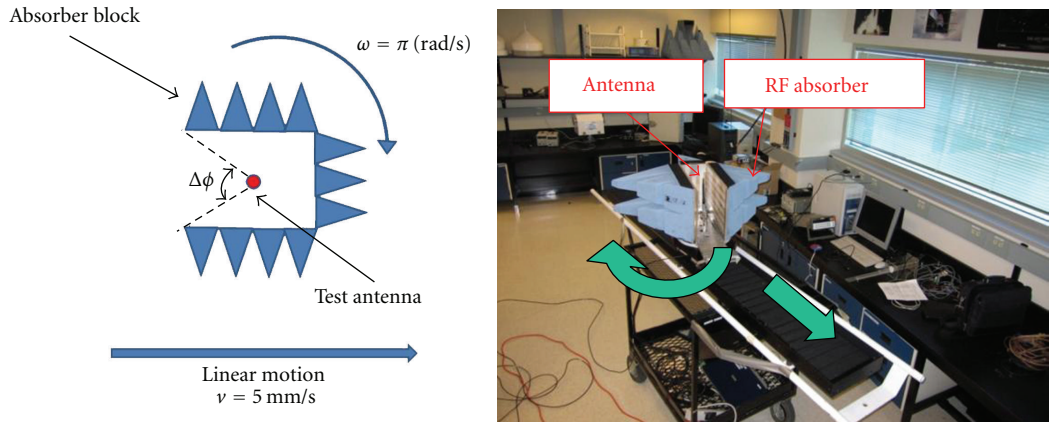

(a) (b)

Figure 2: (a) The arrangement of the absorber block and the antenna in the tests, as seen from the top. The antenna is colocated with the axis of rotation of the absorber block. The height of the absorber block is such that it blocks the direct path signals in the elevation range of $|\theta| < \pi/4$. (b) The measurement equipment.

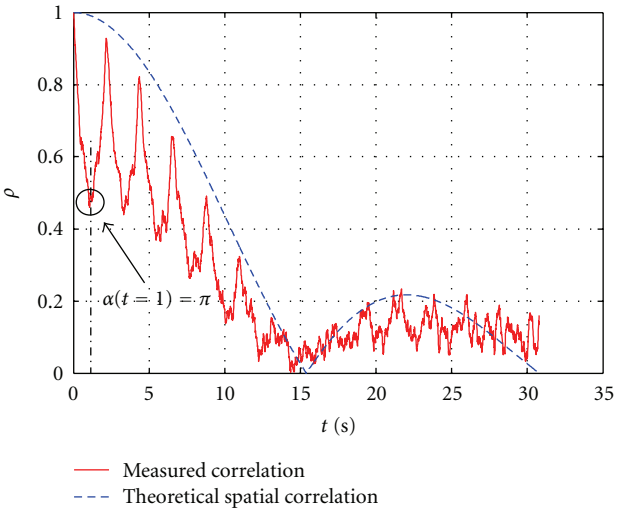

Figure 3: Measured signal correlation as a function of time.

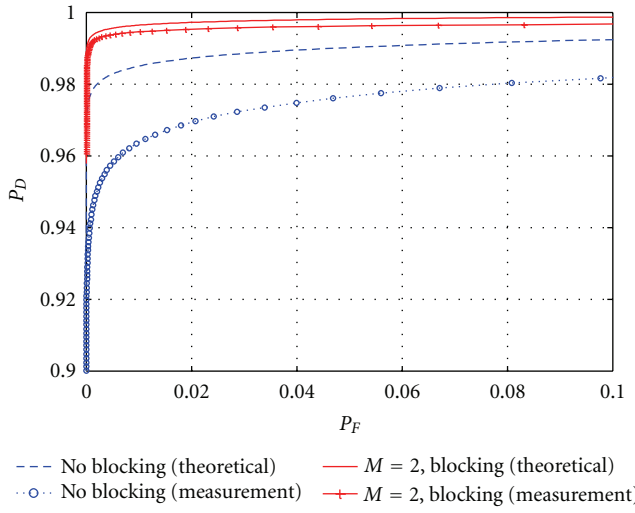

Figure 4: Measured and theoretical ROC curves at $\eta = 21$ dB.

connected to an RF front-end for downconversion, sampling and despreading. A static reference antenna, located several wavelengths away from the test antenna, was used to compensate for the residual oscillator offset and drift. That is the local replica despreading signal was generated based on signal locking to this reference signal. Note that the separation between the static reference antenna and the test antenna varies due to the spatial translation of the test antenna. However, the experiment is set up such that a minimum distance of five wavelengths is maintained between the test and the reference antennas at all times, therefore avoiding the issue of mutual coupling. A block of pyramidal electromagnetic absorbers with absorption over a broad frequency range including the carrier frequency of the CDMA signal was mounted on a rotating table facilitating a circular motion with the test antenna collocated with the axis of rotation of the absorber block. The absorber block's speed of rotation was set to $\omega = \pi$ rad/s. Figure 2 shows the measurement equipment and the absorber-antenna arrangement which in two runs of measurements was based on:

(a) no blocking ($M = 1$),

(b) nearly orthogonal blocking ($\Delta\phi = \pi$, $M = 2$). The height of the absorber block is such that it blocks the direct path signals in the elevation range of $|\theta| < \pi/3$.

The axis of rotation of the absorber structure is coincident with the vertical axis of the dipole antenna. Then combined absorber and antenna are spatially translated based on a precision linear motion table with a constant speed of $v = 5$ mm/s. The range of motion of the linear table is sufficient to obtain 260 spatially uncorrelated sample sets. Hence the experimental apparatus of Figure 2 undergoes compound motion of simultaneous rotation and translation.

The output signal of the test antenna was integrated over $\Delta T = 10$ ms periods. Note that the antenna displacement is negligible in subsequent sampling subintervals therefore complying with the assumption of antenna stationarity. To verify the assumption of signal decorrelation based on antenna blocking, the magnitude of complex correlation coefficient of the antenna output signal was numerically estimated from

$$\rho(t) = \left| \frac{\left\langle \mathbf{x}_i \mathbf{x}_k^* \right\rangle}{\sqrt{\left\langle \mathbf{x}_i \mathbf{x}_i^* \right\rangle \left\langle \mathbf{x}_k \mathbf{x}_k^* \right\rangle}} \right|, \tag{12}$$

where $\langle \cdots \rangle$ is a time average, $t \equiv |i - k|\Delta T$ is time vector and $\mathbf{x}_i$ are the demodulated baseband antenna outputs defined in (5). The measured correlation for scenario (b) is plotted in Figure 3 as a function of time t, which maps into the spatial and angular displacements of the test antenna and the absorber block based on $p(t) = vt$ m, and $\alpha(t) = \omega t$ rad, respectively. As can be seen in the figure, the rotation of the absorber block exposes the test antenna to multipath arriving from different directions resulting in signal decorrelation. An acceptably low signal correlation of $\rho < 0.5$ is observed at $t = 1$ which corresponds to a π radian rotation of the absorber block, for example, an approximately orthogonal blocking. As a result, a set of two weakly correlated signal samples approximately equivalent to a diversity order of two is realized based on the measurement apparatus. This can be exploited to generate useful diversity gain. Note that the scattering objects in the near field of the test antenna violate the assumption of orthogonal blocking and therefore a full signal decorrelation, $\rho \simeq 0$, is not realizable. In addition to blocking, the antenna motion further decorrelates the signal (see Figure 3), and therefore a combination of motion and blocking can be considered to further improve diversity gain.

An SLC was applied to the M = 2 signal samples corresponding to scenario (b), and the resulting ROC curve is plotted in Figure 4 along with the ROC curve resulting from scenario (a). In order to provide a valid comparison, the ROC curve for the scenario (a) was plotted after $T = 2\Delta T = 20$ ms of coherently integrating the received signal corresponding to an average SNR of 21 dB. The theoretical ROC curves are also plotted for comparison, and a good agreement between the measurement and the theoretical results is observed. As is evident from the measured ROC curves, antenna blocking results in a notable improvement in signal detectability. The corresponding processing gain was calculated from (7) and found to be G = 3.1 dB at $P_{F0} = 0.01$ and $\eta = 21$ dB, which is a good match to the theoretical prediction of $G = 3.6$ dB for the same values of SNR and P_{F0}. Note that the antenna is spatially moved as the absorber is being rotated. This of course results in an inflated diversity. However the antenna only moves 0.03 wavelengths for each half rotation of the absorber structure. Hence the spatial contribution to the decorrelation is negligible.

A potential limitation of these measurements is the issue of attaining statistical significance. Experimental results in this paper are based on 260 uncorrelated spatial samples per absorber-antenna arrangement which appears to be adequate based on the results.

5. Conclusion

A counterintuitive diversity gain generating method based on antenna blocking was analyzed and verified as described in this paper. A model based on M orthogonal blocking functions was studied, and through theoretical analysis it was shown that the proposed technique can result in several dBs of processing gain. As is evident from the analysis, where the available average SNR is high, for example, $\eta \geq 15$ dB for a target $P_{F0} = 0.01$, antenna blocking can result in usable processing gain.

A set of measurements was performed in order to validate the theoretical analysis. An agreeable signal decorrelation (<0.5) was observed based on rotating a block of absorbers around a test antenna. A test scenario based on combining $M = 2$ samples was studied, and a processing gain of 3.1 dB was measured. The experimental ROC curves demonstrate the performance of the utilized antenna blocking diversity technique, and the measurement results were found to be in good agreement with the theoretical predictions. The theoretical and the measurement results attest to the effectiveness of the proposed technique for mitigating multipath fading and enhancing signal detectability in indoor multipath environments. Note that the experimental setup in this paper was designed to verify the possibility of achieving diversity gain based on antenna blocking under controlled conditions. The user interaction with the handset is of course random resulting in diversity that is a combination of orientation, translation, and pattern blocking. Hence while this paper emphasizes the potential diversity gain due to blockage, a stochastic model of the user interaction is required for evaluating the statistics of the diversity gain attributable from the blocking perspective.

References

[1] J. S. Colburn, "Evaluation of personal communications dual-antenna handset diversity performance," *IEEE Transactions on Vehicular Technology*, vol. 47, no. 3, pp. 737–746, 1998.

[2] T. S. Rappaport and S. Sandhu, "Radio-wave propagation for emerging wireless personal-communication systems," *IEEE Antennas and Propagation Magazine*, vol. 36, no. 5, pp. 14–24, 1994.

[3] R. G. Vaughan and J. B. Andersen, "Antenna diversity in mobile communications," *IEEE Transactions on Vehicular Technology*, vol. 36, no. 4, pp. 149–172, 1987.

[4] R. G. Vaughan, "Pattern translation and rotation in uncorrelated source distributions for multiple beam antenna design," *IEEE Transactions on Antennas and Propagation*, vol. 46, no. 7, pp. 982–990, 1998.

[5] P. Mattheijssen, M. H. A. J. Herben, G. Dolmans, and L. Leyten, "Antenna-pattern diversity versus space diversity for use at handhelds," *IEEE Transactions on Vehicular Technology*, vol. 53, no. 4, pp. 1035–1042, 2004.

[6] S. L. Preston and D. V. Thiel, "Base-station tracking in mobile communications using a switched parasitic antenna array,"

IEEE Transactions on Antennas and Propagation, vol. 46, no. 6, pp. 841–844, 1998.

[7] S. L. Preston, D. V. Thiel, J. W. Lu, S. G. O'Keefe, and T. S. Bird, "Electronic beam steering using switched parasitic patch elements," *Electronics Letters*, vol. 33, no. 1, pp. 7–8, 1997.

[8] D. V. Thiel, S. G. O'Keefe, and J. W. Lu, "Electronic beam steering in wire and patch antenna systems using switched parasitic elements," in *Proceedings of the IEEE Antennas and Propagation Society, AP-S International Symposium & URSI Radio Science Meeting*, vol. 1, pp. 534–537, Baltimore, Md, USA, 1996.

[9] R. G. Vaughan, "Switched parasitic elements for antenna diversity," *IEEE Transactions on Antennas and Propagation*, vol. 47, no. 2, pp. 399–405, 1999.

[10] M. Pelosi, O. Franek, M. B. Knudsen, M. Christensen, and G. F. Pedersen, "A grip study for talk and data modes in mobile phones," *IEEE Transactions on Antennas and Propagation*, vol. 57, no. 4, pp. 856–865, 2009.

[11] J. Krogerus, J. Toivanen, C. Icheln, and P. Vainikainen, "Effect of the human body on total radiated power and the 3-D radiation pattern of mobile handsets," *IEEE Transactions on Instrumentation and Measurement*, vol. 56, no. 6, pp. 2375–2385, 2007.

[12] K. Ogawa and T. Matsuyoshi, "An analysis of the performance of a handset diversity antenna influenced by head, hand, and shoulder effects at 900 MHz: part I—effective gain characteristics," *IEEE Transactions on Vehicular Technology*, vol. 50, no. 3, pp. 830–844, 2001.

[13] K. Ogawa, T. Matsuyoshi, and K. Monma, "An analysis of the performance of a handset diversity antenna influenced by head, hand, and shoulder effects at 900 MHz. II. Correlation characteristics," *IEEE Transactions on Vehicular Technology*, vol. 50, no. 3, pp. 845–853, 2001.

[14] A. Broumandan, J. Nielsen, and G. Lachapelle, "Signal detection performance in rayleigh fading environments with a moving antenna," *IEEE Signal Processing Transactions*, vol. 4, pp. 117–129, 2010.

[15] A. Broumandan, J. Nielsen, and G. Lachapelle, "Indoor GNSS signal acquisition performance using a synthetic antenna array," *IEEE Transactions on Aerospace and Electronic Systems*, vol. 47, no. 2, pp. 1337–1350, 2011.

[16] V. Dehghanian, J. Nielsen, and G. Lachapelle, "Pattern diversity through azimuth blocking," in *Proceedings of the IEEE International Symposium on Antennas and Propagation (APSURSI '10)*, July 2010.

[17] V. Dehghanian, J. Nielsen, G. Lachapelle, and P. Aflaki, "Diversity gain through synthesizing multiple polarizations," in *Proceedings of the 23rd Canadian Conference on Electrical and Computer Engineering (CCECE '10)*, pp. 1–6, May 2010.

[18] V. Dehghanian, J. Nielsen, and G. Lachapelle, "Combined spatial-polarization correlation function for indoor multipath environments," *IEEE Antennas and Wireless Propagation Letters*, vol. 9, pp. 950–953, 2010.

[19] H. L. VanTrees, *Detection Estimation and Modulation Theory: Part IV*, John Wiley & Sons, New York, NY, USA, 2002.

[20] T. S. Rappaport, *Wireless Communications: Principles and Practice*, Prentice Hall PTR, 2nd edition, 2001.

[21] E. D. Kaplan, *Understanding GPS: Principles and Applications*, Artech House, 2nd edition, 2006.

[22] R. E. Collin and F. J. Zucker, *Antenna Theory*, vol. 4, McGraw-Hill, New York, NY, USA, 1969.

[23] C. A. Balanis, *Antenna Theory*, John Wiley & Sons, New York, NY, USA, 1997.

[24] C. Caini, G. E. Corazza, and A. Vanelli-Coralli, "DS-CDMA code acquisition in the presence of correlated fading—part I: theoretical aspects," *IEEE Transactions on Communications*, vol. 52, no. 7, pp. 1160–1168, 2004.

[25] S. Kay, *Fundamentals of Statistical Signal Processing: Detection Theory*, vol. 2, Printice-Hall, New Jersey, NJ, USA, 1998.

[26] A. Broumandan, J. Nielsen, and G. Lachapelle, "Enhanced detection performance of indoor GNSS signals based on synthetic aperture," *IEEE Transactions on Vehicular Technology*, vol. 59, no. 6, pp. 2711–2724, 2010.